Fish and Shellfish Immunology 166 (2025) 110611

Contents lists available at ScienceDirect

Fish and Shellfish Immunology

journal homepage: www.elsevier.com/locate/fsi

Full length article

Comprehensive analysis of colony-stimulating factor genes and immunostimulatory effects of CSF3a in rainbow trout (*Oncorhynchus mykiss*)

Mengqun Liu, Qiusheng Wang, Ziyi Zhao, Xin Qi, Haishen Wen *

Key Laboratory of Mariculture (Ocean University of China), Ministry of Education (KLMME), Ocean University of China, Qingdao, 266003, PR China

ARTICLE INFO

Keywords:
Colony-stimulating factor family
Rainbow trout
Inflammatory response
Bacterial infection
Cell proliferation

ABSTRACT

Colony-stimulating factors (CSFs) play critical roles in the host response to tissue injury and pathogenic infection. In this study, we conducted a comprehensive genome-wide analysis and identified seven *csf* genes in rainbow trout (*Oncorhynchus mykiss*). Comparative analyses of gene structure, conserved synteny, and protein sequence alignment further supported their annotation and orthology with other vertebrate *csf* genes. Although *csf3* has been identified in several teleost species, its biological functions remain largely uncharacterized. Here, we reported that rainbow trout *csf3* (*Rtcsf3*) genes exhibited broad tissue distribution and were significantly upregulated in response to *Aeromonas salmonicida* infection and pathogen analog stimulation, suggesting their potential role in innate immunity. The open reading frame (ORF) of *csf3a* encodes a 215-amino acid (aa) precursor protein containing a signal peptide and a conserved IL-6-type cytokine domain. Functional assays demonstrated that recombinant CSF3a (rRtCSF3a) significantly increased the expression of inflammatory cytokines (*il1β*, *il10* and *tnfα*) and promoted splenic cell proliferation *in vitro*. Furthermore, transcriptomic profiling of rRtCSF3a-stimulated spleen cells revealed enrichment of genes associated with cytokine signaling, cell proliferation, programmed cell death, and metabolic reprogramming. Collectively, these findings provide the first comprehensive characterization of the *csf* gene family in teleosts and uncover the immunostimulatory and regulatory functions of CSF3a in rainbow trout.

1. Introduction

Colony-stimulating factors (CSFs), members of the cytokine superfamily [1], are glycoproteins with molecular weights between 18 and 70 kDa that regulate the functional activity, survival, proliferation and differentiation of myeloid hematopoietic cells [2,3]. In addition to promoting the maturation of myeloid progenitor cells, CSFs also directly modulate inflammatory and immune responses by acting on mature granulocytes and macrophages [4–8]. The CSF family comprises macrophage colony-stimulating factor (CSF1 or M-CSF), granulocyte-macrophage colony-stimulating factor (CSF2 or GM-CSF), and granulocyte colony-stimulating factor (CSF3 or G-CSF) [9].

CSF1 is the primary regulator of macrophage survival, proliferation, and differentiation [10,11]. It is essential for maintaining tissue homeostasis, enhancing early defense mechanisms against pathogens, modulating downstream immunological responses, and facilitating tissue repair [12]. *Csf1/mcsf* has been identified in several teleost fish species, including rainbow trout (*Oncorhynchus mykiss*), zebrafish (*Danio rerio*), Japanese flounder (*Paralichthys olivaceus*), starry flounder (*Platichthys stellatus*), and goldfish (*Carassius auratus*) [13–18]. Unlike birds and mammals, which possess a single, alternatively spliced *csf1* gene, several teleosts exhibit two distinct *csf1* genes, designated *csf1.1* and *csf1.2* (also referred to as *mcsf1* and *mcsf2*) [19,20]. Wang et al. (2008) cloned two mcsf/*csf1* genes from rainbow trout and demonstrated that recombinant MCSF1 significantly upregulated the expression of the chemokine receptor CXCR3.

CSF2 stimulates mature neutrophils to exhibit chemotaxis, enhances their oxidative metabolism, promotes antibody-dependent phagocytosis and microbial killing, and regulates the production of various regulatory proteins [3]. Additionally, CSF2 is essential in both innate and adaptive immunity, making it a promising therapeutic target for various inflammatory diseases [21–24]. However, CSF2 is absent in the zebrafish genome [25], and no research has reported the existence of CSF2 in other fish species.

* Corresponding author.
E-mail address: wenhaishen@ouc.edu.cn (H. Wen).

https://doi.org/10.1016/j.fsi.2025.110611
Received 3 April 2025; Received in revised form 18 July 2025; Accepted 28 July 2025
Available online 29 July 2025

CSF3 primarily targets polymorphonuclear granulocytes, promoting their proliferation, priming them for host defense, and enhancing their functional maturation. Beyond its role as a hematopoietic growth factor, CSF3 also acts as a key modulator of anti-infective and inflammatory responses [26–28]. Currently, two gene duplications of *csf3* (*csf3a* and *csf3b*) have been characterized in various teleosts, including fugu (*Takifugu rubripes*), pufferfish (*Tetraodon nigroviridis*), black rockfish (*Sebastes schlegelii*), rock bream (*Oplegnathus fasciatus*), large yellow croaker (*Larimichthys crocea*), goldfish (*Carassius auratus* L.), and zebrafish [29–36]. Additionally, four duplications of *csf3* (*gcsfa1*, *gcsfa2*, *gcsfb1* and *gcsfb2*) have been discovered in common carp (*Cyprinus carpio* L.) [37]. Functional analyses in fish indicate that both CSF3a and CSF3b are essential for the normal development of neutrophils and can drive excessive neutrophil production in a CSF3R-dependent manner in zebrafish [25,30,38,39]. Furthermore, infections caused by Salmonellosis and Shigellosis lead to increased *csf3a* mRNA expression in zebrafish, correlating with the induction of a granulopoietic response [25,40,41]. Likewise, the differential regulation of *csf3a* and *csf3b* in response to *Vibrio alginolyticus* or Poly (I:C) in large yellow croaker suggests that these genes may play distinct roles in immune responses [29,31]. However, data on the functions of CSF3 in the innate immune responses of teleosts remain largely unexplored.

In this study, the CSF family was characterized in rainbow trout, an economically important fish species worldwide [42]. The expression patterns of CSF3 following pathogen infection were examined, and its expression modulation was investigated in immune-related tissues and cells. Moreover, the impact of recombinant rainbow trout CSF3a (rRtCSF3a) protein on the expression of inflammatory cytokine genes and the proliferation of spleen cells was examined. These findings enhance the understanding of the characteristics of the CSF family and the biological roles of teleost CSF3 in innate immune regulation.

2. Materials and methods

2.1. Ethics statement

All treatments and experimental manipulations on rainbow trout strictly followed the guidelines established by the Animal Research and Ethics Committee of Ocean University of China (Permit Number: 2014201). The fish utilized in this study were juvenile and sexually immature, so sex-specific effects were not considered.

2.2. CSF gene family

2.2.1. Genome-wide identification of csf genes in rainbow trout

To systematically identify *csf* genes in rainbow trout, protein sequences of known *csf* genes from human (*Homo sapiens*) and zebrafish (*Danio rerio*) were retrieved from the NCBI and Ensembl databases and used as queries for a TBLASTN search (E-value $= 1 \times 10^{-5}$) against the rainbow trout reference genome (GCA_013265735.3). Candidate genes were annotated and further validated by BLASTP searches against the NCBI non-redundant (NR) protein database. ORFs were predicted using the NCBI ORF Finder tool, and the theoretical isoelectric point (pI) and molecular weight (MW) of the putative CSF proteins in rainbow trout were calculated using the ExPASy ProtParam tool.

2.2.2. Phylogenetic, syntenic, and sequence analyses of csf genes

To validate the annotation and evolutionary relationships of putative *csf* gene paralogs in rainbow trout, phylogenetic analysis was performed using MEGA 7.0 with the neighbor-joining method and Jones–Taylor–Thornton model, supported by 1000 bootstrap replicates. Amino acid sequences from representative vertebrates were included to infer orthology, and gene names in rainbow trout were assigned based on sequence similarity to known CSF homologs in other species. To further support gene annotation, syntenic relationships were analyzed by integrating genomic data from the NCBI and Genomicus v92.01 databases. Synteny was examined by comparing genomic neighborhoods surrounding *csf* genes across multiple species, including human, chicken (*Gallus gallus*), zebrafish, American shad (*Alosa sapidissima*), and Atlantic cod (*Gadus morhua*). Additionally, exon–intron structures of the rainbow trout *csf* genes were retrieved from genome annotations and visualized using GSDS 2.0. Conserved protein domains were predicted with the SMART tool, while ten conserved motifs were identified using MEME and visualized via TBtools. Multiple sequence alignments were performed using Clustal X2, and alignment features were graphically represented with ESPript 3.0.

2.3. Fish and challenge experiments

Juvenile rainbow trout (approximately 8 cm in length and 10 g in weight) were sourced from a trout farm in Linqu (Weifang, China). For the bacterial challenge, fish were randomly allocated into the control and the infected group. The infected group consisted of two biological replicates, each containing 20 individuals. Based on our previous study [43], trout in the infected group received an intraperitoneal injection with 0.2 mL of *Aeromonas salmonicida* suspension (1×10^8 CFU/mL), while fish in the control group received an equal volume of sterile phosphate-buffered saline (PBS). Subsequently, at 0, 6, 12, 24, and 48 h post-infection, fish from both groups were euthanized using MS-222. Brain, head kidney, trunk kidney, spleen, liver, and intestine were collected, immediately snap-frozen in liquid nitrogen, and stored at −80 °C for further analysis.

2.4. Transcriptomic analysis following bacterial infection

To examine *csf* gene expression across various tissues in response to bacterial infections, publicly available transcriptomic datasets from our previous studies [44–46], deposited in the NCBI Sequence Read Archive under accession numbers PRJNA867038, PRJNA866872, PRJNA866205, PRJNA865462, and PRJNA753277, were analyzed. Briefly, transcriptomes of brain and kidney tissues were derived from control and infected rainbow trout challenged with *A. salmonicida* [44]. Similarly, RNA-Seq data from gill, intestine, and liver tissues were obtained from both control and symptomatic individuals following *V. anguillarum* infection [46].

Clean reads were aligned to the rainbow trout reference genome using Hisat2 (v2.2.1) [47]. Gene expression levels were quantified with FeatureCounts [48] as raw counts and normalized to fragments per kilobase of transcript per million mapped reads (FPKM) for downstream analysis. Differential expression analysis was conducted with the DESeq2 R package [49]. Genes with an adjusted p-value <0.05 and an absolute $\log_2$ fold change greater than 1 were defined as differentially expressed genes (DEGs). Gene Ontology (GO) and Kyoto Encyclopedia of Genes and Genomes (KEGG) pathway enrichment analyses were performed for the identified DEGs using the hypergeometric distribution algorithm to identify significantly enriched functional categories and biological pathways [50].

2.5. Gene cloning and construction of a prokaryotic expression vector

The ORF of RtCSF3a was amplified via PCR with gene-specific primers (RtCSF3a-F, RtCSF3a-R; Table S1), which were designed according to the predicted coding sequence of RtCSF3a. The PCR template consisted of first-strand cDNA synthesized from total RNA extracted from the brain of rainbow trout. The resulting amplicon was ligated into the pCE2 TA/Blunt Zero Vector (Vazyme, China) using TOPO cloning method. The recombinant plasmid was verified by Sanger sequencing to ensure sequence accuracy.

2.6. Expression and purification of recombinant RtCSF3a

Based on transcriptomic analysis (Fig. S1), the *csf3a* gene showed

consistent upregulation across multiple bacterial infection models, while maintaining basal expression. In contrast, other *csf* family members displayed limited or inconsistent responsiveness. Therefore, *Rtcsf3a* was selected as a representative immune-relevant candidate for recombinant protein expression and functional analysis. To produce recombinant RtCSF3a protein (rRtCSF3a), the coding sequence was amplified using gene-specific primers (PE-CSF3a-F, PE-CSF3a-R; Table S1) and ligated into the pET-32a(+) expression vector. The full sequence information of the recombinant plasmids used is presented in Supplementary Fig. S2. The resulting recombinant plasmid was transformed into *Escherichia coli* Rosetta gamiB (DE3) cells (Ang Yu, China). Positive clones were cultured in Luria-Bertani (LB) medium with 2 g/L glucose (Sigma-Aldrich, USA), 100 mg/L ampicillin (Sigma-Aldrich), and 34 mg/L chloramphenicol (Sangon Biotech, China) at 37 °C.

Upon reaching an optical density at 600 nm (OD_{600}) of 0.4, the bacterial culture was rapidly cooled in an ice bath. A 10 mL aliquot of the culture was collected as a control sample for total bacterial protein before induction. The sample was centrifuged at 3500×*g* for 5 min, and the bacterial pellet was retained. The pellet was resuspended in lysis buffer (500 mM NaCl, 20 mM phosphate buffer, 10 mM imidazole) to obtain the total protein before induction. To the remaining culture, isopropyl-β-D-thiogalactopyranoside (IPTG; Sigma-Aldrich) was added to achieve a final concentration of 0.3 mM to induce protein expression. Cultures were subsequently incubated at 16 °C for 12 h. Following induction, bacterial cells were harvested by centrifugation at 3500×*g* for 10 min at 4 °C. The cell pellets were resuspended in lysis buffer and lysed via sonication on ice. The lysates were clarified by centrifugation at 12,000×*g* for 10 min at 4 °C, with the supernatant retained for further processing.

Recombinant proteins were purified from the supernatant using Ni-NTA affinity chromatography (Beyotime Biotechnology, China). To prepare the gravity column, pack it with NTA-Ni resin and pre-equilibrate it with PBS by filling the column, opening the outlet, and allowing the liquid to flow through completely. Repeat this washing step twice to ensure proper equilibration. The supernatant from the lysed bacterial suspension was filtered through 0.22 μm sterilizing membranes and loaded onto the pre-equilibrated column. The column was then incubated on ice with gentle shaking for 1 h to facilitate binding of the recombinant protein to the resin. After incubation, drain the liquid from the column, referred to as the flowthrough. The column was subsequently washed thoroughly by filling it with washing buffer (500 mM NaCl, 20 mM phosphate buffer, 40 mM imidazole) and releasing the liquid. This washing process, which produced washing buffer fractions, was repeated eight times to remove non-specifically bound proteins. The target protein was then eluted from the column using an elution buffer (500 mM NaCl, 20 mM phosphate buffer, 250 mM imidazole). The elution process was repeated four times, and all fractions were combined to obtain the purified target protein. The eluent containing the target protein was transferred to a dialysis bag and placed in a beaker containing pre-cooled 1 × PBS. The solution was gently stirred with a magnetic stirrer and dialyzed on ice for 12 h to remove excess salts and imidazole. Following dialysis, the protein solution was filtered through 0.22 μm sterilizing membranes, aliquoted, rapidly frozen in liquid nitrogen, and stored at −80 °C for preservation. Protein concentrations were determined using a BCA assay kit (Beyotime Biotechnology), and the expression levels were analyzed through SDS-PAGE.

2.7. Splenic primary cell culture, stimulation, and functional assays

Healthy rainbow trout were anesthetized and dissected to collect spleen tissues, which were rinsed in PBS supplemented with 1 % penicillin–streptomycin–gentamicin solution (Absin, China) to remove residual blood. The tissues were finely minced and enzymatically digested using Trypsin-EDTA solution (Biosharp, China) at a tissue-to-buffer volume ratio of 1:3. To facilitate dissociation, the suspension was gently pipetted using a sterile Pasteur pipette (Biosharp, China) and incubated for 20 min. Digestion was terminated by adding an equal volume of complete L-15 medium containing 10 % fetal bovine serum (FBS; Absin, China) and 1 % antibiotics to neutralize residual trypsin activity. The resulting cell suspension was filtered through 40-μm sterile nylon meshes (BD, USA) to remove tissue debris and centrifuged at 400×*g* for 5 min, and cell concentration and viability were assessed using 0.2 % trypan blue exclusion. Samples with viability >95 % were resuspended in complete L-15 medium and seeded into 6-, 12-, or 96-well culture plates. Cells were incubated at 18 °C for 24–48 h to allow adherence. Non-adherent cells (primarily red blood cells and dead cells) were removed by gently replacing the medium with FBS-free L-15 containing antibiotics only. Adherent cells were then starved in this medium for an additional 6 h prior to stimulation.

For pathogen analogue stimulation assays, cells seeded in 12-well plates were stimulated with lipopolysaccharide (LPS) or polyinosinic: polycytidylic acid [Poly(I:C)] at a final concentration of 40 μg/mL. PBS-treated cells served as the control. All treatments were performed in triplicate, with three biological replicates per group. Cells were harvested at 3, 6, and 12 h post-stimulation for total RNA extraction, followed by cDNA synthesis for quantitative real-time PCR (qPCR) analysis.

For the cell proliferation assay, primary splenic cells were seeded into 96-well plates and treated with purified rRtCSF3a protein at final concentrations of 0, 10, 100, or 1000 ng/mL. Each treatment group included four technical replicates and was repeated in three independent biological experiments. After 48 h of incubation at 18 °C, 10 μL of CCK-8 reagent (Beyotime Biotechnology, China) was added to each well and incubated for an additional 2 h according to the manufacturer's instructions. Care was taken to avoid bubble formation. Cell proliferation was assessed by measuring optical density at 450 nm.

For transcriptomic analysis following rRtCSF3a stimulation, primary splenic cells were seeded into 6-well plates and treated with purified rRtCSF3a protein at a final concentration of 100 ng/mL. Cells treated with an equivalent volume of PBS served as the control group. All treatments were performed in triplicate, with three biological replicates per group. Cells were harvested 6 h post-stimulation for total RNA extraction, which was subsequently subjected to bulk RNA sequencing to investigate the transcriptomic response to rRtCSF3a.

2.8. Expression analysis of RtCSF3 genes by qPCR

qPCR was conducted using a StepOnePlus™ Real-Time PCR System (Applied Biosystems, USA) with *β-actin* utilized as the internal reference gene [44]. The primer information used for qPCR analysis of *csf3* paralogs and cytokine genes (*il1β*, *tnfα*, *il10*) is provided in Table S1. Each 10 μL reaction contained 1 μL cDNA, 5 μL SYBR® FAST qPCR Master Mix, 0.2 μL of both forward and reverse primers, and 3.6 μL of RNase-free water. The thermal cycling protocol was as follows: 95 °C for 30 s, followed by 40 cycles of 95 °C for 10 s and 60 °C for 30 s, 72 °C for 30 s. Relative mRNA expression levels were determined utilizing the $2^{-\Delta\Delta CT}$ method [51].

2.9. Statistical analysis

Statistical analyses were performed using SPSS 21.0 (IBM Corp., USA). One-way ANOVA was conducted to assess *Rtcsf3* gene expression across tissues (Fig. 3), as well as the effects of *A. salmonicida* infection and pathogen analogue stimulation on *Rtcsf3* expression (Figs. 4 and 5). Additionally, one-way ANOVA was used to analyze splenic cell proliferation induced by rRtCSF3a treatment (Fig. 7). When the assumption of homogeneity of variances was met, Fisher's Least Significant Difference (LSD) post hoc test was applied; otherwise, Dunnett's T3 test was used. Independent-samples t-tests were performed to compare the expression of immune-related cytokines between rRtCSF3a-treated and control groups at each time point (Fig. 7). Results are presented as the means ± standard error of the mean (SEM), with differences deemed significant at

$p < 0.05$.

3. Result

3.1. Identification of the csf genes in rainbow trout

Seven *csf* genes were found in the rainbow trout genome and categorized into two subgroups: CSF1/M-CSF and CSF3/G-CSF. Previously, Wang et al. (2008) identified two *csf1* genes in rainbow trout: *mcsf1* (i.e., *csf1a2*) and *mcsf2* (i.e., *csf1b2*). However, with the availability of improved genome assemblies, we identified two additional *csf1* genes from a newly sequenced genome (GCA_013265735.3). The detailed characteristics of *csf* genes are summarized in Table 1, with CSF2/GM-CSF absent in rainbow trout. The lengths of the identified *csf* genes ranged from 1191 to 4136 bp, encoding proteins of 205–629 amino acids (aa), with predicted molecular weights (MW) of 19.58–69.64 kDa and isoelectric points (pI) from 5.16 to 7.69.

3.2. Phylogenetic and syntenic analysis of csf genes

To confirm the annotation of rainbow trout *csf* genes and elucidate their phylogenetic relationships, the phylogenetic tree was constructed utilizing amino acid sequences from 53 *csf* genes across rainbow trout and representative vertebrate species. As shown in Fig. 1A, rainbow trout *csf* genes clustered with their homologs in corresponding subgroups and were classified into two subgroups: *csf1/mcsf* and *csf3/gcsf*. This result supports the classification of the trout *csf* genes and provides a foundation for their accurate identification and annotation in rainbow trout. In addition, the rainbow trout *csf* genes were mapped to chromosomes (Fig. 1B). The seven *csf* genes were unevenly distributed across six chromosomes.

To further validate gene annotations, particularly for genes with multiple paralogs, syntenic analysis was performed (Fig. 1C and D). The results showed that the rainbow trout *csf1a/b* genes share highly conserved neighboring genes with the *csf1a/b* genes of zebrafish, Atlantic cod, and American shad, while the rainbow trout *csf3* genes share conserved neighbors with the *csf3* genes of human, chicken, and zebrafish. In Fig. 1C, conserved genes neighboring *csf1a* include *golt1a*, *plekha6*, and *atp2b2*, while those neighboring *csf1b* include *ren*, *mapkapk2*, *slc12a5b*, *magi1a/2*, and *eif2d*. In Fig. 1D, conserved genes neighboring *csf3a* include *rara*, *gjd3*, *top2a*, *med24*, and *lrrc3c*, with *lrrc3c* also conserved among genes neighboring *csf3b1/b2*. These findings provide strong support for the annotation of rainbow trout *csf* genes and indicate that *csf* genes have remained relatively conserved throughout evolution.

3.3. Gene structure analyses of csf genes

To investigate structural divergence within the *csf* gene family, structural domain analysis was performed (Fig. 2A). The exon-intron structures of *csf3* genes are relatively conserved in position and number, whereas *csf1* exhibits greater variation. Within the *csf1* subgroup, *csf1a1* and *csf1a2* each contain 10 exons, while *csf1b1* has one fewer exon than *csf1b2*. In *csf3* subgroup, *csf3a*, *csf3b1*, and *csf3b2* all contain five exons. Additionally, all CSF proteins contain two conserved motifs, motifs 4 and 6 (Fig. 2B). The four CSF1 proteins contain six conserved motifs (motifs 6-1-2-3-4-7), while the three CSF3 proteins (CSF3a, CSF3b1, and CSF3b2) contain three conserved motifs (motifs 6-4-5). Notably, CSF3 protein possesses an additional motif (motif 5) compared to the motif pattern in CSF1. Furthermore, CSF1a includes three additional motifs (motifs 10-9-8) compared to CSF1b. These distinct motifs may contribute to the functional differentiation of CSF proteins. Collectively, the observed differences in gene structure and motif reflect the evolutionary diversification and potential functional diversity of CSFs in rainbow trout.

3.4. Multiple sequence alignment analysis of CSFs

The deduced RtCSF1 protein shares a similar structure with human CSF1, comprising a signal peptide, a conserved CSF1 domain, and a transmembrane region [13], despite variations in protein size among species and the relatively low homology between teleost and mammalian CSF1 (Fig. 2C). The variations in protein size are primarily due to differences in the length of the region separating the CSF1 domain and the transmembrane domain among different molecules, which often include regions of low compositional complexity [13]. Additionally, sequence alignment revealed the conservation of residues in rainbow trout that are critical for CSF1 function in mammals, including cysteine residues that form intrachain disulfide bonds ("*SS*") and histidine residues that interact with CSF1R, as predicted based on human CSF1 [13,52,53]. Furthermore, two cysteine residues implicated in interchain disulfide bridge formation are preserved in RtCSF1a1 and RtCSF1a2. Meanwhile, the cysteine residues critical for interchain disulfide bond formation in mammalian CSF1 are also conserved in RtCSF1a2, RtCSF1b1, and RtCSF1b2.

The deduced rainbow trout CSF3 (RtCSF3) protein exhibits a secondary structure resembling that of human CSF3, characterized by a four-α-helix bundle with a left-handed twist [29,54], despite their low sequence identity (Fig. 2D). The four cysteine residues responsible for forming two disulfide bonds in mammals and birds are not conserved in rainbow trout RtCSF3. The cysteine residue potentially involved in disulfide bond (SS") formation is retained in RtCSF3b1 and RtCSF3b2, but is absent in RtCSF3a. Notably, all RtCSF3 isoforms preserve a conserved IL-6-type cytokine domain.

3.5. Expression analysis of Rtcsf3 in tissues and primary cells following pathogen stimulation

In the *V. anguillarum* infection model (Figs. S1C, D, E), *Rtcsf3* genes (*csf3a*, *csf3b1*, and *csf3b2*) were significantly upregulated ($p < 0.01$) in both gill and intestine. In contrast, *Rtcsf1* genes (*csf1a1*, *csf1a2*, *csf1b1*, and *csf1b2*) did not exhibit statistically significant expression changes ($p > 0.05$) under either *V. anguillarum* or *A. salmonicida* infection (Fig. S1A and B). These findings prompted us to focus on the *Rtcsf3* genes, which showed stronger immune responsiveness. Tissue distribution analysis revealed that the *Rtcsf3* genes were broadly expressed across six examined tissues. *Rtcsf3a* was most highly expressed in the brain and spleen (Fig. 3A), whereas *Rtcsf3b1* showed peak expression levels in the liver and spleen (Fig. 3B). Similarly, *Rtcsf3b2* was most prominently expressed in the liver (Fig. 3C). Following *A. salmonicida* challenge,

Table 1
Sequence characteristics of *csf* genes identified in rainbow trout.

Gene name		Gene ID	Location	Chr	Protein length (aa)	MW (kDa)	pI	mRNA (bp)
csf1/mcsf	*csf1a1*	110528367	70082033.70113471	7	629	69.64	6.25	4136
	csf1a2	100136089	51601433.51640412	17	593	65.74	5.98	2891
	csf1b1	110533011	34715740.34721316	9	273	31.03	5.68	1191
	csf1b2	100301638	60412147.60416804	16	276	31.12	5.16	1773
csf3/gcsf	*csf3a*	110491561	20082548.20085438	16	215	23.60	5.36	1577
	csf3b1	100499617	33335447.33339727	13	205	19.58	6.83	1820
	csf3b2	110538077	66674135.66678665	12	205	22.55	7.69	2355

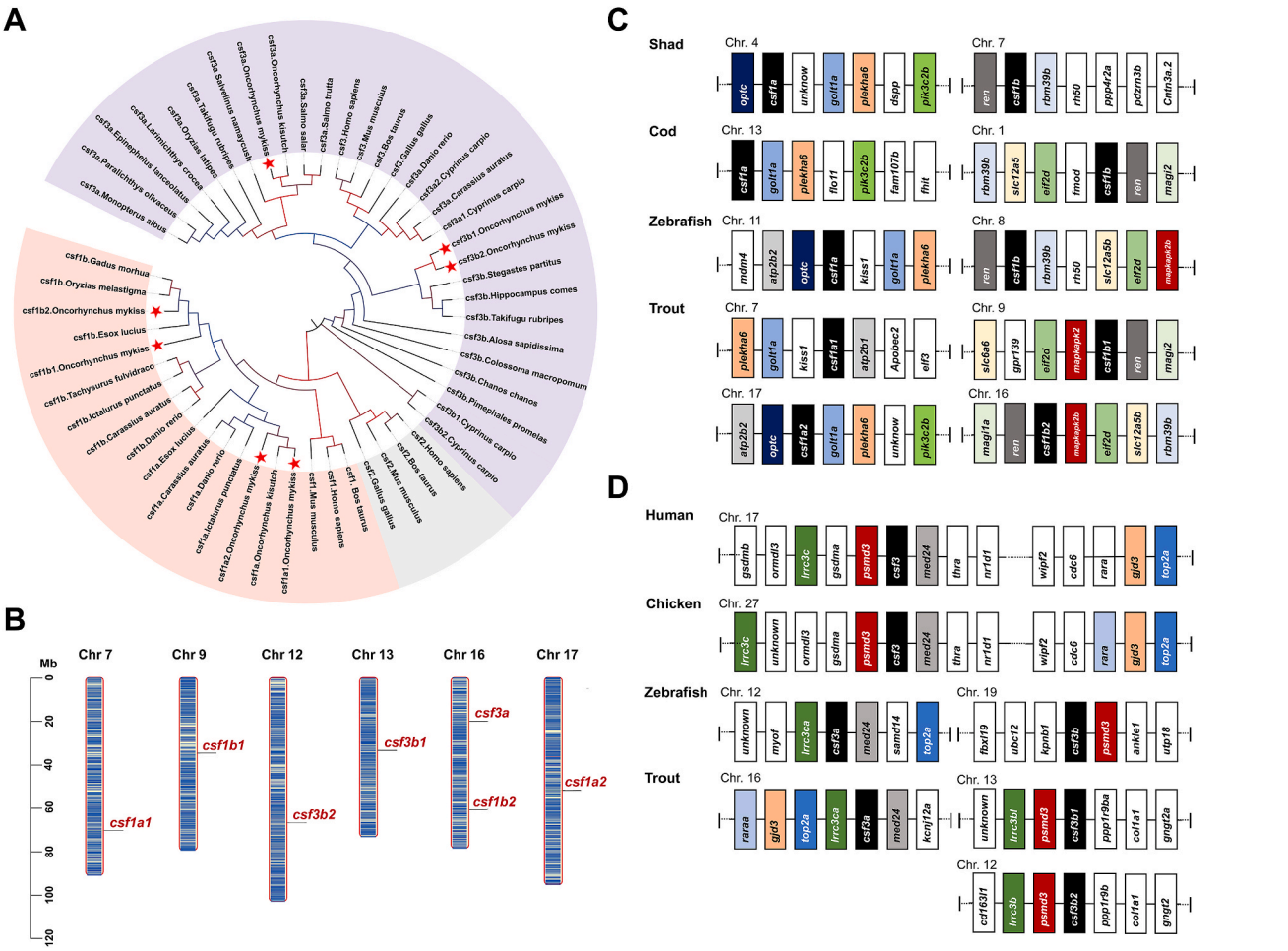

Fig. 1. (A) Phylogenetic tree of *csf* genes from rainbow trout and representative vertebrate species. *Csf* genes from rainbow trout are marked with red five-pointed stars. Three circular color blocks on the evolutionary tree are marked as *csf1*, *csf2*, and *csf3* respectively. (B) Chromosome (Chr) locations of rainbow trout *csf* genes mapped to the reference genome. The depth of shading on each chromosome reflects gene density, and horizontal lines indicate the physical positions of *csf* genes. (C, D) Syntenic analysis of *csf1* (C) and *csf3* (D) genes across multiple species. Colored blocks denote conserved homologous genes. Abbreviations: Mb, Megabase pairs; Chr, Chromosome; Shad, American shad; Cod, Atlantic cod; Trout, rainbow trout.

Rtcsf3a expression in the spleen was markedly upregulated, reaching a 16-fold peak at 12 h post-injection (hpi) (Fig. 4A). Similarly, *Rtcsf3b1* and *Rtcsf3b2* were significantly induced, with peak expression levels of 1.6-fold (Figs. 4B) and 6.7-fold (Fig. 4C), respectively, also observed at 12 hpi. These results indicate that RtCSF3 may participate in the immune defense response of rainbow trout against pathogen infection.

To examine the influences of pathogen analog stimulation on *Rtcsf3* gene expression *in vitro*, primary spleen cells were treated with LPS and Poly (I:C). *Rtcsf3a* expression was significantly upregulated by LPS, reaching a peak at 6 h with approximately a 10-fold upregulation, whereas Poly (I:C) had no significant effect (Fig. 5A). In contrast, *Rtcsf3b1* expression was rapidly induced by both stimuli, peaking at 3 h with 11.4-fold and 4-fold increases following LPS and Poly (I:C) treatment, respectively (Fig. 5B). *Rtcsf3b2* expression was significantly elevated by LPS, peaking at 6 h with an 8.8-fold increase, while Poly (I:C) elicited no significant response (Fig. 5C).

3.6. Characterization of RtCSF3a

The deduced RtCSF3a protein consists of 215 aa, including a 17-aa signal peptide (MNILIVFAILCNMASYG) and a 198-aa mature peptide (Fig. 6B). It harbors a conserved 156-aa IL-6 domain, a characteristic feature of fish homologs (Fig. 6B). The secondary structure of RtCSF3a closely resembles that of human and zebrafish CSF3 (four α-helices and a short helix) [30,54] (Fig. 2D). Phylogenetic analysis revealed that RtCSF3a clusters with other fish CSF3a homologs (Figs. 1A and 6A). Additionally, synteny analysis demonstrated that CSF3a exhibits a highly conserved genomic arrangement across vertebrates, with the *lrrc3ca* gene positioned upstream and the *med24* gene positioned downstream (Fig. 1D). Collectively, these conserved features confirm that the identified gene encodes a CSF3a homologue in rainbow trout.

3.7. Bioactivity of rRtCSF3a and its effect on cell proliferation

CSF3 is known to modulate the expression of immune-related genes [55,56]. We hypothesized that the influence of rRtCSF3a on bacterial infection might be partially mediated through its immunoregulatory role. To test this hypothesis, recombinant rRtCSF3a was expressed, purified (Supplementary Fig. S3), and used to stimulate primary spleen cells isolated from rainbow trout. The results demonstrated that rRtCSF3a significantly upregulated the expression of *il1β* (NM_001124347.2), *il10* (NM_001245099.1) and *tnfα* (NM_001124357.1) at both 6 and 12 h post-stimulation (Fig. 7A–C). These findings suggest that rRtCSF3a possesses immunoregulatory properties.

To examine the effect of rRtCSF3a on the proliferation of splenic cells, primary spleen cells were incubated with varying concentrations of rRtCSF3a, while PBS served as the control. Cell proliferation was assessed via MTT assay. Treatment with 100 ng/mL rRtCSF3a significantly enhanced cell proliferation relative to the PBS control (Fig. 7D).

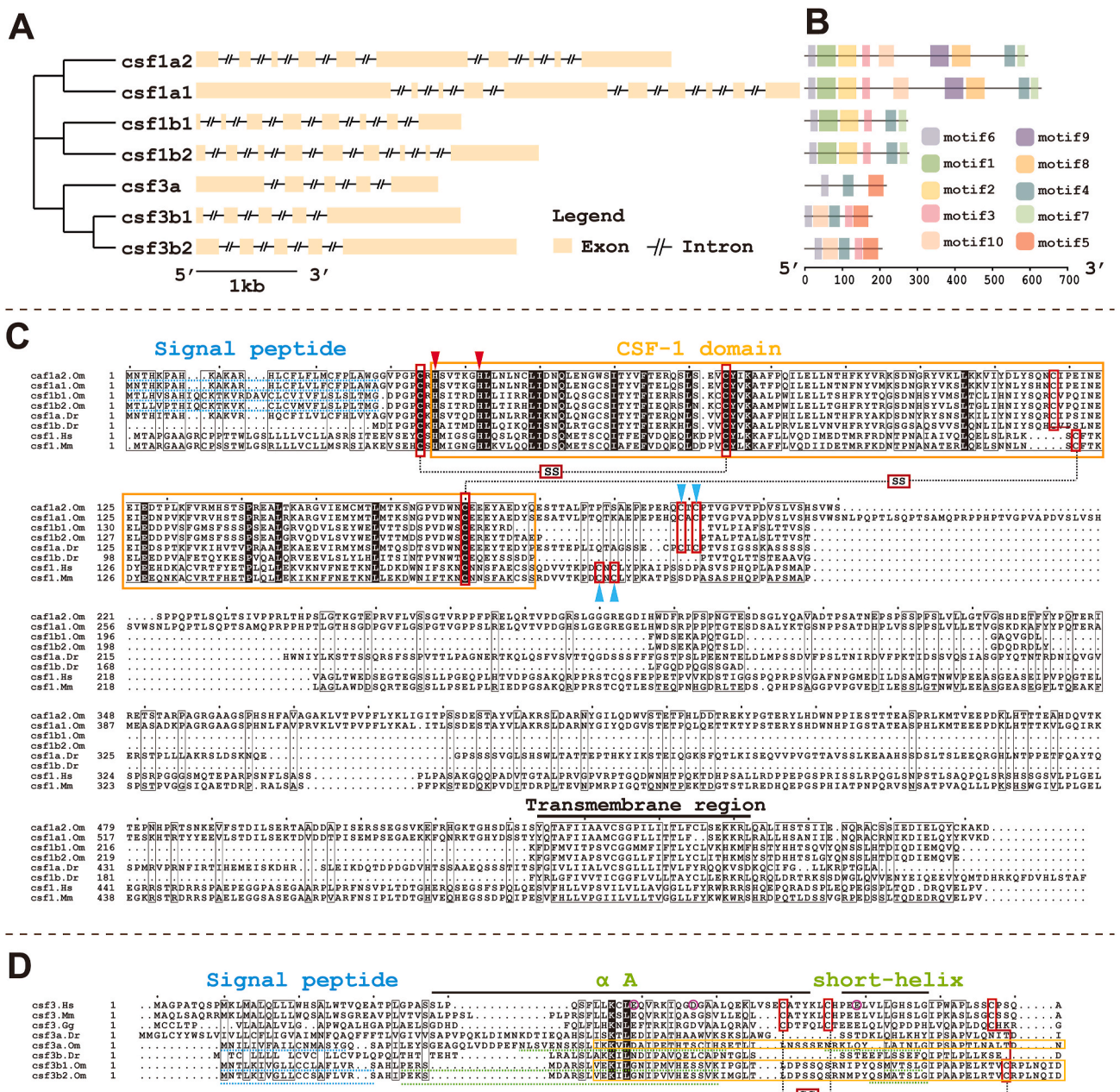

Fig. 2. (A) Exon–intron structures and (B) conserved motif compositions of *csf* genes in rainbow trout. Distinct motifs are depicted in different colors. Multiple sequence alignments of vertebrate (C) CSF1 and (D) CSF3 amino acid sequences are shown. Identical residues (highlighted in black) and similar residues (outlined in black boxes) were identified using ClustalW. Signal peptide sequences are underlined with blue dotted lines. In rainbow trout CSF1, the predicted conserved CSF-1 domain is indicated by an orange box. Conserved cysteine residues forming disulfide bonds ("SS") are marked with red boxes, while histidine residues critical for CSF1R interaction are marked with red arrows. Two cysteine residues involved in interchain disulfide bridge formation are indicated with blue arrows. In trout CSF3, the predicted conserved IL-6 domains are indicated by orange boxes. Predicted helices (αA to αD and the short helix) are underlined with green dotted lines. Glutamic acid "E" and aspartic acid "D" residues that represent key binding interfaces with CSF3R are circled in purple. Structural annotations and predicted features are partially based on Katakura et al. (2019). Species abbreviations: Om, *Oncorhynchus mykiss*; Hs, *Homo sapiens*; Mm, *Mus musculus*; Gg, *Gallus gallus*; Dr, *Danio rerio*.

However, a higher concentration (1000 ng/mL) led to a partial inhibition of proliferation. This post-optimal suppression is consistent with previous *in vitro* studies in rainbow trout, which suggest receptor saturation or desensitization as possible mechanisms underlying diminished responsiveness at elevated cytokine concentrations [57,58].

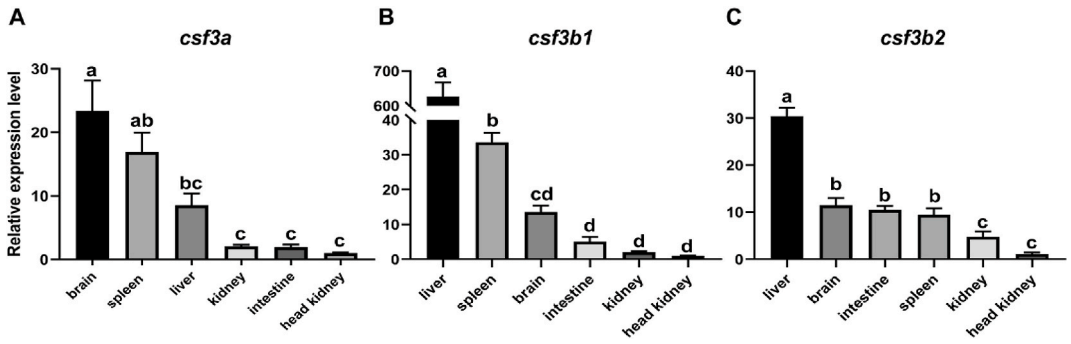

Fig. 3. Tissue-specific expression of *csf3* paralogs in rainbow trout: (A) *csf3a*, (B) *csf3b1*, and (C) *csf3b2*. Gene expression levels in the head kidney were used as internal controls to calculate the relative expression of *csf3* genes. Data are presented as means ± SEM. Different lowercase letters indicate statistically significant differences among tissues ($p < 0.05$).

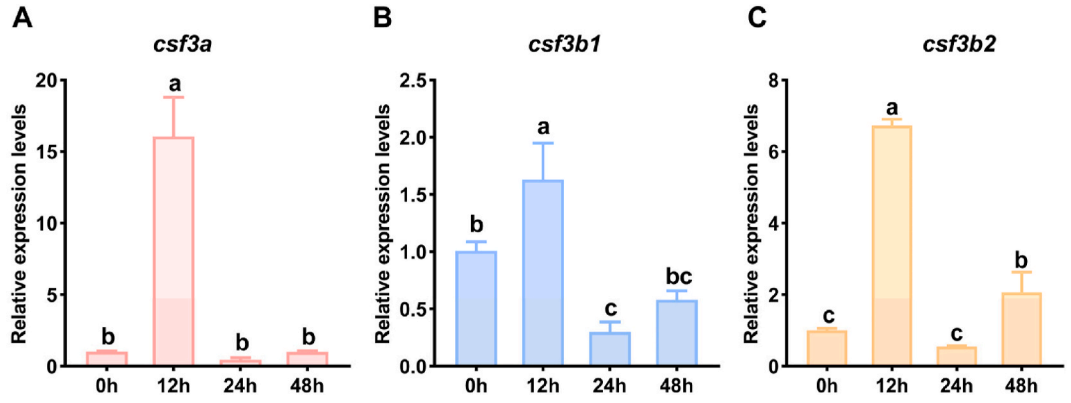

Fig. 4. Effects of *A. salmonicida* challenge on *csf3* mRNA relative expression levels in the spleen of rainbow trout at different time points. (A) *csf3a*; (B) *csf3b1*; (C) *csf3b2*. Results are presented as means ± SEM. Different lowercase letters indicate statistically significant differences in expression levels in the spleen ($p < 0.05$).

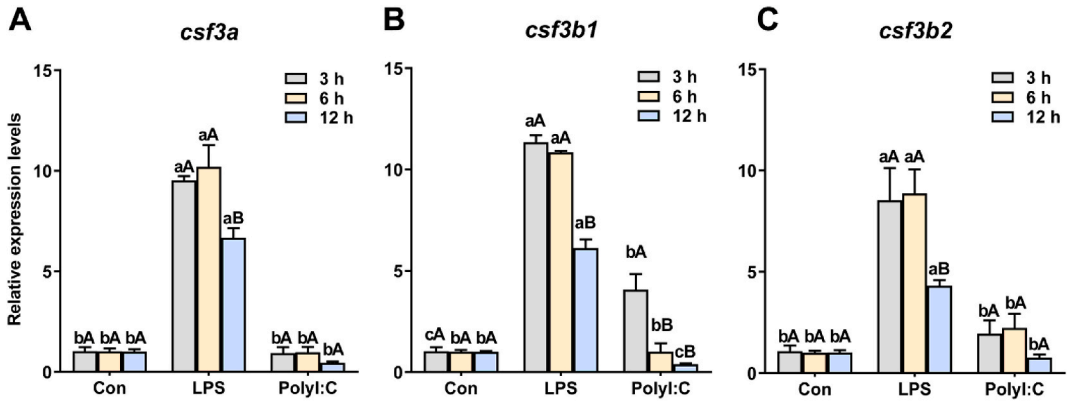

Fig. 5. Relative expression levels of *csf3* in primary spleen cells of rainbow trout following stimulation with LPS or Poly (I:C). (A) *csf3a*; (B) *csf3b1*; (C) *csf3b2*. Results are presented as the means ± SEM. Different lowercase letters denote significant differences between treatments at the same time point ($p < 0.05$). Different uppercase letters indicate significant differences ($p < 0.05$) across time points within the same treatment.

3.8. Identification of DEGs

RNA-seq was performed on six spleen cell samples collected following rRtCSF3a stimulation, generating a total of 142.42 million raw reads. After quality filtering, 132.64 million high-quality clean reads were retained. Detailed sequencing statistics are provided in Table S2. The proportion of clean reads mapped to the rainbow trout reference genome ranged from 92.82% to 94.38%, with an average mapping rate of 93.57%. The RNA-seq data have been deposited in the NCBI Sequence Read Archive under accession number PRJNA1291363. Differential expression analysis between the rRtCSF3a-treated and control groups identified a total of 393 differentially expressed genes (DEGs) (Fig. 8). Among them, 356 genes were upregulated and 37 genes were downregulated following rRtCSF3a stimulation.

3.9. Enrichment analysis of DEGs

GO enrichment analysis (Fig. 9A; Table S3) revealed that rRtCSF3a stimulation significantly upregulated genes associated with immune-related biological processes and molecular functions. The top 20 enriched GO terms included *inflammatory response* (GO:0006954), *cellular response to lipopolysaccharide* (GO:0071222), *immune response*

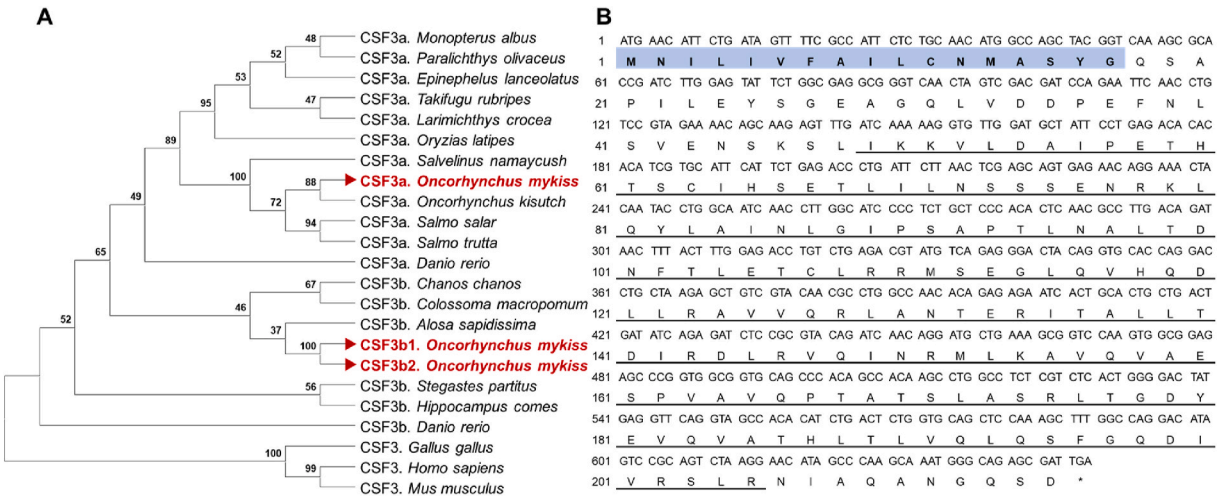

Fig. 6. (A) Phylogenetic tree of CSF3 from rainbow trout and representative vertebrate species. CSF3 sequences from rainbow trout are indicated by red triangles. Bootstrap values shown at the branches represent confidence levels of the phylogenetic relationships. (B) Nucleotide and deduced amino acid sequences of rainbow trout *csf3a*. The predicted signal peptide sequence, identified using SignalP 5.0, is marked with blue shading. The conserved IL-6 homologue domain is underlined.

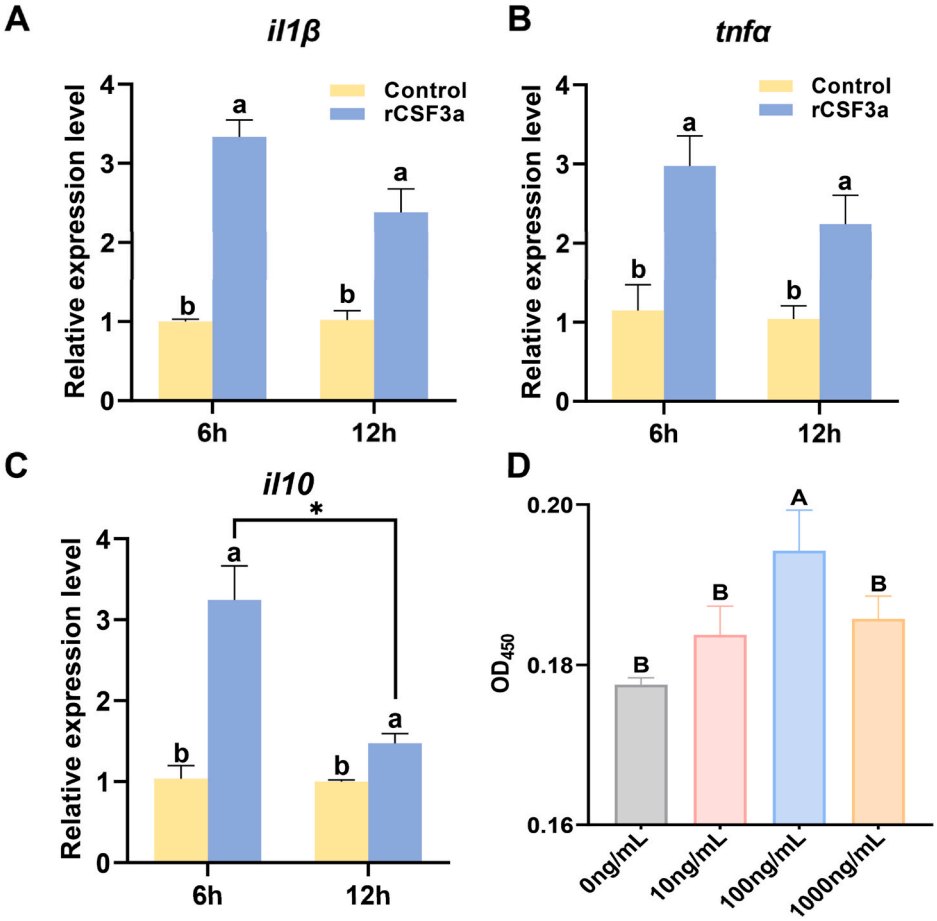

Fig. 7. Effects of recombinant RtCSF3a (rRtCSF3a) on the expression of immune-related cytokines and the proliferation of rainbow trout spleen cells. (A–C) Expression levels of *il1β* (A), *tnfα* (B), and *il10* (C) in primary spleen cells after incubation with PBS (control) or rCSF3a for 6 and 12 h. (D) Cell proliferation measured after 48-h incubation with increasing concentrations of rRtCSF3a (0, 10, 100, and 1000 ng/mL). Values are presented as means ± SEM. An asterisk (✱) denotes a statistically significant difference ($p < 0.05$) in expression levels after rRtCSF3a treatment at different time points. Different lowercase or uppercase letters indicate significant differences ($p < 0.05$) among treatment groups within the same time point.

(GO:0006955), *regulation of cell population proliferation* (GO:0042127), *cytokine activity* (GO:0005125), *defense response to bacterium* (GO:0042742), *innate immune response* (GO:0045087), and *leukocyte chemotaxis involved in inflammatory response* (GO:0002232), among others.

KEGG pathway enrichment analysis (Fig. 9B) further demonstrated

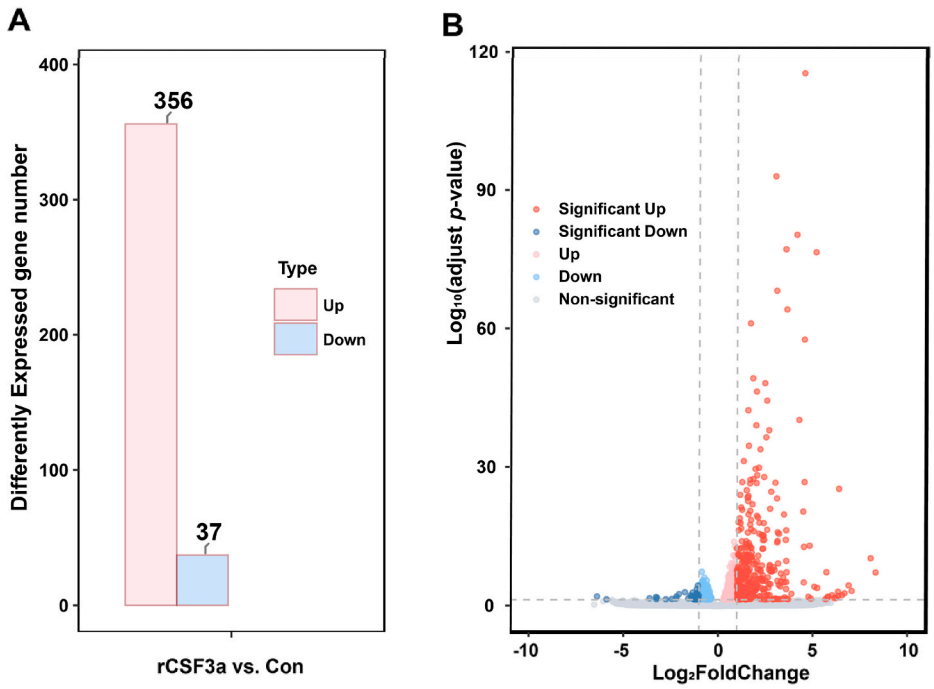

Fig. 8. (A) Number of differentially expressed genes (DEGs) identified in primary spleen cells following rRtCSF3a stimulation. (B) Volcano plot showing the distribution of DEGs in response to rRtCSF3a stimulation.

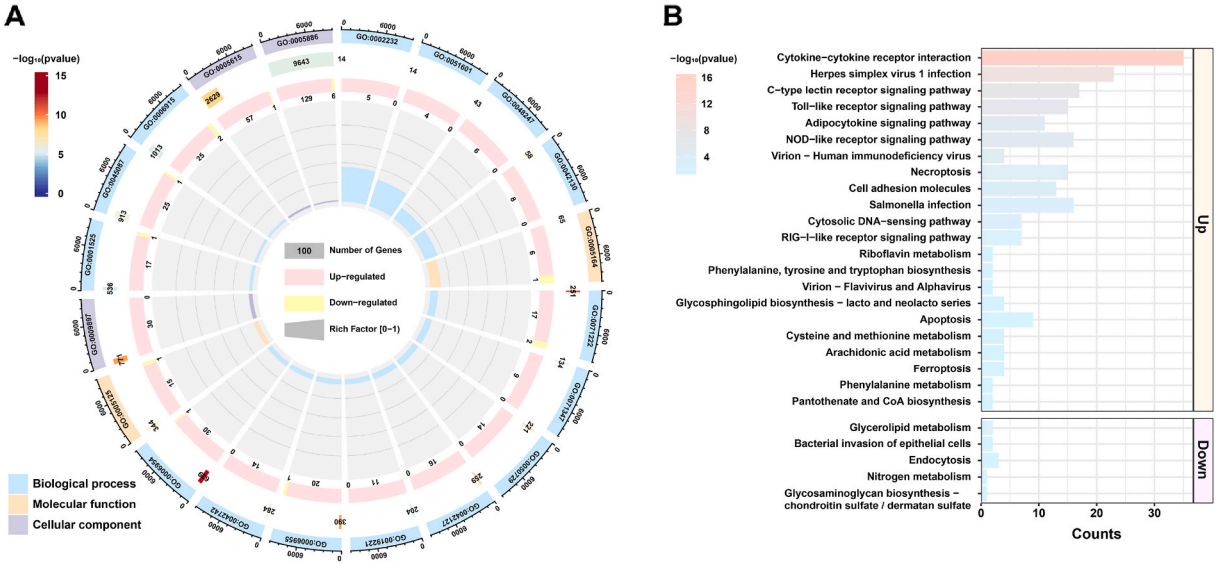

Fig. 9. (A) GO enrichment analysis. The outermost circle displays the enriched GO terms with the number of associated genes indicated by the scale. Different colors distinguish the functional classifications. The second circle represents the number of background genes and corresponding *p*-values, where bar length shows gene count and color indicates significance (red = lower *p*-value, blue = higher *p*-value). The third circle illustrates the proportion of upregulated (pink) and downregulated (yellow) DEGs for each term. Numerical values are displayed at the bottom of each bar. The innermost circle shows the RichFactor (the ratio of DEGs to background genes), with gridlines spaced at 0.2 intervals. (B) KEGG pathway enrichment analysis. The color intensity of each rectangle represented the significance of enrichment.

that DEGs were predominantly involved in key immune signaling pathways, including *cytokine-cytokine receptor interaction*, pattern recognition receptor pathways such as *Toll-like*, *NOD-like*, and *RIG-I-like receptor signaling*, and programmed cell death processes including *apoptosis*, *necroptosis*, and *ferroptosis*. These results suggest that rRtCSF3a stimulation leads to the activation of innate immune signaling and modulation of cell survival pathways. In addition, several metabolic pathways, including *riboflavin metabolism* and *arachidonic acid metabolism,* were also enriched. In contrast, downregulated pathways were mainly related to lipid metabolism and intracellular transport processes, such as *glycerolipid metabolism* and *endocytosis*. These changes may reflect a reallocation of cellular resources during immune stimulation.

4. Discussion

4.1. Repertoire of csf gene family in rainbow trout

CSFs are crucial to the host response to tissue damage and

pathogenic infection [59–62]. However, the characteristics and functions of the *csf* gene family in rainbow trout have not been comprehensively examined. This study provides the first thorough identification of *csf* genes in rainbow trout, revealing seven *csf* genes, classifying them into two distinct subgroups, and highlighting an expansion in *csf* gene copies compared to higher vertebrates. Their annotations were further validated through phylogenetic analysis, sequence structure analysis, and syntenic analysis. Additionally, the expanded *csf1* (*csf1a1*, *csf1a2*, *csf1b1* and *csf1b2)* and *csf3* (*csf3a*, *csf3b1* and *csf3b2*) paralogs were distributed on distinct chromosomes, rather than co-localized on the same chromosome as tandem duplications, indicating that they originated from three rounds (3R) or four rounds (4R) of whole-genome duplication (WGD) events [30,63,64]. Gene duplication is a major evolutionary force driving the emergence of novel functional genes involved in diverse biological processes, thereby contributing to potential functional diversification of *csf* gene family in rainbow trout [65].

Additionally, we found that *csf2* was also absent in rainbow trout, similar to its absence in zebrafish. Following genome evolution in the teleost fish (3R), many individual genes or gene clusters were lost in zebrafish, including a missing *il3* family gene cluster, as well as the absence of ligands and receptors for *il3*, *il5*, and *csf2* [66]. Conversely, these cytokines are indispensable in birds and mammals for maintaining myelomonocytic lineages. The loss of *csf2* in zebrafish likely indicates compensatory adaptations by functionally redundant or neo-functionalized genes derived from WGD [30,66]. Similarly, the absence of *csf2* in rainbow trout is most likely compensated by functional genes derived from WGD. These findings provide a more comprehensive understanding of the *csf* gene repertoire in salmonids and lay the foundation for further functional studies in rainbow trout.

4.2. Biological information of CSF3 in rainbow trout

Phylogenetic analyses showed that CSF3 is distinctly clustered into one branch in fish and another in higher vertebrates (Fig. 6A). Structural and sequence analysis of *csf3* revealed that three *csf3* copies (*csf3a*, *csf3b1*, and *csf3b2*) in rainbow trout retain the gene structure of *csf3* in human, mouse (*Mus musculus*), and other teleost fish [18,36,37,67]. Rainbow trout CSF3 exhibits a signal peptide, four α-helices, a short helix, and a conserved IL-6 domain, similar to CSF3 in human and common carp [37]. Additionally, they share specific acidic residues, such as glutamate and aspartate, which are implicated in ligand-receptor binding [37], suggesting that RtCSF3 has been relatively conserved throughout evolution and that RtCSF3 genes are homologs of mammalian CSF3.

4.3. Expression dynamics and functional divergence of csf3 paralogs

CSF3 is a key cytokine that regulates the proliferation, survival, and differentiation of neutrophils, monocytes, macrophages, and their progenitors while also serving an essential function in antimicrobial immunity [56,68–71]. CSF3 is widely distributed across mammals, birds, and teleost fish. Initially purified and described in mouse [72], it was subsequently identified in non-mammalian vertebrates, including chicken [33], African clawed frog (*Xenopus laevis*) [73], and various teleost species [13,36,37,67]. In mammals, multiple inflammatory stimuli, such as increased pro-inflammatory cytokines and LPS, significantly induce CSF3 production [74]. In teleosts, similar immune induction has been reported: for instance, in black rockfish, *gcsf1* expression levels in peripheral blood leukocytes were significantly upregulated by LPS and Poly (I:C) [32]. In rock bream, infection with *Streptococcus iniae* significantly elevated *gcsf1* and *gcsf2* expression in the kidneys, spleen, and gills, while *Edwardsiella tarda* infection led to significant upregulation of *gcsf2* in the kidney [34]. In Japanese flounder, challenges with *V. anguillarum*, *E. tarda*, and infectious spleen and kidney necrosis virus (ISKNV) significantly induced the expression of *gcsf/csf3* transcripts in the brain, kidney, spleen, and liver [56]. Consistently, *Rtcsf3* expression is significantly upregulated in the spleen at 12 h after *in vivo* injection of *A. salmonicida*. Furthermore, *Rtcsf3* expression was significantly induced *in vitro* primary spleen cells stimulated by LPS at 3, 6, and 12 h. These findings indicate that CSF3 is crucial to the immune response of rainbow trout against pathogenic infections. Interestingly, *Rtcsf3a* and *Rtcsf3b1* exhibited distinct expression patterns following Poly (I:C) stimulation, implying functional divergence between these paralogs. Similar differential expression of *csf3a* and *csf3b* has also been observed in large yellow croaker with *V. alginolyticus* or Poly (I:C) [29,31], further supporting that these paralogs may play distinct roles in the immunological response.

4.4. Immunostimulatory activity and transcriptomic effects of rRtCSF3a

Previous studies in mammals have demonstrated that recombinant CSF3 enhances neutrophil function and reduces bacterial loads during *Listeria monocytogenes* infection [56,75–77]. Similarly, in teleosts, recombinant CSF3 has been shown to promote immune cell proliferation via pathways such as JAK-STAT signaling [15]. Consistent with these findings, we observed that treatment with rRtCSF3a significantly stimulated the proliferation of rainbow trout splenic primary cells, aligning with results reported in large yellow croaker and common carp [15,37]. These results underscore the conserved immunostimulatory function of CSF3 across vertebrate species.

To further elucidate the mechanism of rRtCSF3a action, we performed transcriptomic profiling of primary spleen cells following stimulation. GO enrichment revealed that DEGs were significantly enriched in immune-related processes, including *inflammatory response*, *cytokine activity*, *leukocyte chemotaxis*, and *regulation of cell population proliferation*. These enriched terms are consistent with the observed rRtCSF3a-induced cellular proliferation and immune activation. Moreover, KEGG pathway analysis showed strong activation of key innate immune signaling pathways mediated by Toll-like receptors, NOD-like receptors, and RIG-I-like receptors, all of which are important for pathogen recognition and antimicrobial defenses [78–85].

Beyond immune activation, rRtCSF3a also influenced gene expression related to cell fate regulation and metabolism. DEGs were significantly enriched in pathways associated with programmed cell death, including apoptosis, necroptosis, and ferroptosis. These findings suggest that rRtCSF3a may participate in regulating immune cell turnover, which aligns with the known roles of mammalian CSF3 in apoptosis and cellular homeostasis [86,87]. In addition, enrichment of metabolic pathways suggests a potential involvement of rRtCSF3a in immunometabolic regulation. Collectively, these results support the hypothesis that rRtCSF3a exerts broad immunomodulatory effects by promoting cytokine expression, regulating cell proliferation, modulating immune signaling cascades, and potentially altering cellular metabolic states to support immune activation. Although these *in vitro* findings provide strong evidence for the immunostimulatory capacity of rRtCSF3a, further *in vivo* studies are necessary to confirm its antimicrobial activity under both pathogen-challenged and uninfected conditions.

In conclusion, this study provides the first comprehensive characterization of the *csf* gene family in rainbow trout, identifying seven members, including duplicated *csf1* and *csf3* paralogs. Comparative genomic analyses supported their annotation and evolutionary conservation. Tissue expression profiling revealed broad distribution of *Rtcsf3* genes, with *csf3a*, *csf3b1*, and *csf3b2* significantly upregulated in the spleen following *A. salmonicida* infection. The distinct transcriptional responses of *csf3a* and *csf3b1* to pathogen analogs suggest potential functional divergence between these paralogs. Functional assays demonstrated that rRtCSF3a significantly induced inflammatory cytokine expression and promoted the proliferation of splenic cells. Transcriptomic analysis further revealed enrichment of immune-related pathways, including Toll-like receptor, NOD-like receptor, RIG-I-like receptor signaling, as well as pathways associated with cytokine

activity, cell proliferation, and regulated cell death. Additionally, metabolic pathways enrichment suggests a possible role for rRtCSF3a in immunometabolic adaptation. Together, these findings underscore the immunomodulatory role of CSF3a in rainbow trout and provide molecular insights into the function of CSF3 in teleost immunity.

CRediT authorship contribution statement

Mengqun Liu: Writing-original draft, Data curation, Methodology, Software, Visualization. Qiusheng Wang: Visualization, Investigation. Ziyi Zhao: Visualization, Investigation. Xin Qi: Formal analysis, Writing–review and editing, Validation, Supervision. Haishen Wen: Conceptualization, Validation, Writing–review and editing, Funding acquisition, Project administration.

Funding

This work was supported by the National Natural Science Foundation of China [3217210108] and Shandong Provincial Key Research and Development Program (Major Scientific and Technological Innovation Project) [2022ZLGX01].

Declaration of competing interest

None.

Appendix A. Supplementary data

Supplementary data to this article can be found online at https://doi.org/10.1016/j.fsi.2025.110611.

Data availability

Data will be made available on request.

References

[1] A.C. Ward, Cytokine receptors in development, homeostasis and disease, Int. J. Mol. Sci. 24 (2023).
[2] D.C. Dale, Colony-stimulating factors for the management of neutropenia in cancer patients, Drugs 62 (2002) 1–15.
[3] D. Metcalf, The colony-stimulating factors and cancer, Nat. Rev. Cancer 10 (2010) 425–434.
[4] K. Di Gregoli, J.L. Johnson, Role of colony-stimulating factors in atherosclerosis, Curr. Opin. Lipidol. 23 (2012) 412–421.
[5] J.A. Hamilton, Colony-stimulating factors in inflammation and autoimmunity, Nat. Rev. Immunol. 8 (2008) 533–544.
[6] T.S. McCormick, R.B. Hejal, L.O. Leal, M.A. Ghannoum, GM-CSF: orchestrating the pulmonary response to infection, Front. Pharmacol. 12 (2022).
[7] A. Kumar, A. Taghi Khani, A. Sanchez Ortiz, S. Swaminathan, GM-CSF: a double-edged sword in cancer immunotherapy, Front. Immunol. 13 (2022).
[8] S. Yadav, A. Priya, D.R. Borade, R. Agrawal-Rajput, Macrophage subsets and their role: co-relation with colony-stimulating factor-1 receptor and clinical relevance, Immunol. Res. 71 (2023) 130–152.
[9] A.J. Malbon, E. Michalopoulou, M.L. Meli, E.N. Barker, S. Tasker, K. Baptiste, A. Kipar, Colony stimulating factors in early feline infectious peritonitis virus infection of monocytes and in end stage feline infectious peritonitis; a combined *In vivo* and *in vitro* approach, Pathogens 9 (2020) 1–22.
[10] L. An, J. Michaeli, P. Pallavi, A. Breedijk, X. Xu, N. Dietrich, M. Sigl, M. Keese, K. Nitschke, J. Jarczyk, et al., Concurrent stimulation of monocytes with CSF1 and polarizing cytokines reveals phenotypic and functional differences with classical polarized macrophages, J. Leukoc. Biol. 112 (2022) 437–447.
[11] S.K. Sinha, A. Miikeda, Z. Fouladian, M. Mehrabian, C. Edillor, D. Shih, Z. Zhou, M. K. Paul, S. Charugundla, R.C. Davis, et al., Local M-CSF (Macrophage colony-stimulating factor) expression regulates macrophage proliferation and apoptosis in atherosclerosis, Arterioscler. Thromb. Vasc. Biol. 41 (2021) 220–233.
[12] A.M. Rieger, P.C. Hanington, M. Belosevic, D.R. Barreda, Control of CSF-1 induced inflammation in teleost fish by a soluble form of the CSF-1 receptor, Fish Shellfish Immunol. 41 (2014) 45–51.
[13] T. Wang, P.C. Hanington, M. Belosevic, C.J. Secombes, Two macrophage colony-stimulating factor genes exist in fish that differ in gene organization and are differentially expressed, J. Immunol. 181 (2008) 3310–3322.
[14] T. Wang, T. Kono, M.M. Monte, H. Kuse, M.M. Costa, H. Korenaga, T. Maehr, M. Husain, M. Sakai, C.J. Secombes, Identification of IL-34 in teleost fish: differential expression of rainbow trout IL-34, MCSF1 and MCSF2, ligands of the MCSF receptor, Mol. Immunol. 53 (2013) 398–409.
[15] H. Gu, B. Wang, J. He, Y. Hu, Macrophage colony stimulating factor (MCSF) of Japanese flounder (*Paralichthys olivaceus*): immunoregulatory property, anti-infectious function, and interaction with MCSF receptor, Dev. Comp. Immunol. 116 (2021).
[16] M. Gouife, Z. Ban, X. Yue, J. Jiang, J. Xie, Molecular characterization, gene expression and functional analysis of goldfish (*Carassius auratus* L.) macrophage colony stimulating factor 2, Front. Immunol. 14 (2023).
[17] M. Hason, T. Mikulasova, O. Machonova, A. Pombinho, T.J. van Ham, U. Irion, C. Nüsslein-Volhard, P. Bartunek, O. Svoboda, M-CSFR/CSF1R signaling regulates myeloid fates in zebrafish via distinct action of its receptors and ligands, Blood Adv. 6 (2022) 1474–1488.
[18] M.-Y. Sohn, G. Kang, K.-H. Kim, H.-J. Son, C.-I. Park, Molecular adjuvant potential of GCSF and MCSF in starry flounder challenged with *Streptococcus parauberis*, Animals (2025) 15.
[19] B.A. Katzenback, F. Katakura, M. Belosevic, Goldfish (*Carassius auratus* L.) as a model system to study the growth factors, receptors and transcription factors that govern myelopoiesis in fish, Dev. Comp. Immunol. 58 (2016) 68–85.
[20] R. Sinha, Macrophage: a key player of teleost immune system, in: V. Kumar (Ed.), Macrophages - Celebrating 140 Years of Discovery, IntechOpen, Rijeka, 2022. ISBN 978-1-80355-625-3.
[21] I.P. Wicks, A.W. Roberts, Targeting GM-CSF in inflammatory diseases, Nat. Rev. Rheumatol. 12 (2016) 37–48.
[22] I. Joshi, W.P. Carney, E.P. Rock, Utility of monocyte HLA-DR and rationale for therapeutic GM-CSF in sepsis immunoparalysis, Front. Immunol. 14 (2023).
[23] F. Ingelfinger, D. De Feo, B. Becher, GM-CSF: master regulator of the T cell-phagocyte interface during inflammation, Semin. Immunol. 54 (2021) 101518.
[24] K.A.M. Mills, F. Westermann, V. Espinosa, E. Rosiek, J. V Desai, M.A. Aufiero, Y. Guo, F.L. Liu, K.A. Mitchell, S. Tuzlak, et al., GM-CSF–mediated epithelial-immune cell cross-talk orchestrates pulmonary immunity to *Aspergillus fumigatus*, Sci. Immunol. 10 (2025) eadr0547.
[25] V. Pazhakh, G.J. Lieschke, Hematopoietic growth factors: the scenario in zebrafish, Growth Factors 36 (2018) 196–212.
[26] T. Hartung, S. Von Aulock, A. Wendel, Role of granulocyte colony stimulating factor in infection and inflammation, Med. Microbiol. Immunol. 187 (1998) 61–69.
[27] J. Wang, J. Wang, Neutrophils, functions beyond host defense, Cell. Immunol. 379 (2022) 104579.
[28] A.B. Meier, F. Basheer, R. Sertori, M. Laird, C. Liongue, A.C. Ward, Granulocyte colony-stimulating factor mediated regulation of early myeloid cells in zebrafish, FBL 27 (2022) 110–null.
[29] Q. Li, Y. Chen, L. Xu, Y. Yang, Q. Wen, L. Gu, J. Ao, X. Chen, Identification and bioactivity of a granulocyte colony-stimulating factor a homologue from large yellow croaker (*Larimichthys crocea*), Fish Shellfish Immunol. 98 (2020) 167–175.
[30] D.L. Stachura, O. Svoboda, C.A. Campbell, R. Espín-Palazón, R.P. Lau, L.I. Zon, P. Bartůněk, D. Traver, The zebrafish granulocyte colony-stimulating factors (Gcsfs): 2 paralogous cytokines and their roles in hematopoietic development and maintenance, Blood 122 (2013) 3918–3928.
[31] Q. Li, L. Xu, J. Ao, C. Ai, X. Chen, Identification and bioactivity of a granulocyte colony-stimulating factor b homologue from large yellow croaker (*Larimichthys crocea*), Fish Shellfish Immunol. 90 (2019) 20–29.
[32] B.H. Nam, G.H. An, G.W. Baeck, M.C. Kim, J.W. Kim, H.J. Park, D.C. Lee, C. Il Park, Molecular cloning and expression of cDNAs for two distinct granulocyte colony stimulating factor genes from black rockfish *Sebastes schlegelii*, Fish Shellfish Immunol. 27 (2009) 360–364.
[33] M.D. Santos, M. Yasuike, I. Hirono, T. Aoki, The granulocyte colony-stimulating factors (CSF3s) of fish and chicken, Immunogenetics 58 (2006) 422–432.
[34] C. Il Park, J.M. Jeong, J.D. Shim, J.S. Bae, Protective responses of two paralogs of granulocyte colony stimulating factor (GCSF) in rock bream, *Oplegnathus fasciatus* during bacterial and viral infection, Fish Shellfish Immunol. 65 (2017) 206–212.
[35] J. Zou, C.J. Secombes, The function of fish cytokines, Biology 5 (2016).
[36] M. Gouife, F. Wang, Z. Ban, X. Yue, J. Jiang, J. Xie, Molecular and functional characterization of two granulocyte colony stimulating factors in goldfish (*Carassius auratus* L.), Comp. Biochem. Physiol., Part B: Biochem. Mol. Biol. 268 (2023) 110879.
[37] F. Katakura, K. Nishiya, A.S. Wentzel, E. Hino, J. Miyamae, M. Okano, G. F. Wiegertjes, T. Moritomo, Paralogs of common carp granulocyte colony-stigmulating factor (G-CSF) have different functions regarding development traffickingand activation of neutrophils, Front. Immunol. 10 (2019) 1–18.
[38] M.-C. Keightley, C.-H. Wang, V. Pazhakh, G.J. Lieschke, Delineating the roles of neutrophils and macrophages in zebrafish regeneration models, Int. J. Biochem. Cell Biol. 56 (2014) 92–106.
[39] C. Liongue, C.J. Hall, B.A. O'Connell, P. Crosier, A.C. Ward, Zebrafish granulocyte colony-stimulating factor receptor signaling promotes myelopoiesis and myeloid cell migration, Blood 113 (2009) 2535–2546.
[40] C.J. Hall, M.V. Flores, S.H. Oehlers, L.E. Sanderson, E.Y. Lam, K.E. Crosier, P. S. Crosier, Infection-responsive expansion of the hematopoietic stem and progenitor cell compartment in zebrafish is dependent upon inducible nitric oxide, Cell Stem Cell 10 (2012) 198–209.
[41] A.R. Willis, V. Torraca, M.C. Gomes, J. Shelley, M. Mazon-Moya, A. Filloux, C. Lo Celso, S. Mostowy, *Shigella*-induced emergency granulopoiesis protects Zebrafish Larvae from secondary infection, mBio 9 (2018) 1–10.
[42] E. D'Agaro, P. Gibertoni, S. Esposito, Recent trends and economic aspects in the Rainbow Trout (*Oncorhynchus mykiss*) sector, Appl. Sci. (2022) 12.
[43] C. Zeng, Z.S. Hou, H.K. Zhao, Y.R. Xin, M.Q. Liu, X.D. Yang, H.S. Wen, J.F. Li, Identification and characterization of caspases genes in rainbow trout

(*Oncorhynchus mykiss*) and their expression profiles after *Aeromonas salmonicida* and *Vibrio anguillarum* infection, Dev. Comp. Immunol. 118 (2021) 103987.
[44] M. Liu, X. Yang, C. Zeng, H. Zhao, J. Li, Z. Hou, H. Wen, Transcriptional signatures of immune, neural, and endocrine functions in the brain and kidney of Rainbow Trout (*Oncorhynchus mykiss*) in response to *Aeromonas salmonicida* infection, Int. J. Mol. Sci. 23 (2022) 1–17.
[45] Q. Yang, X.D. Yang, M.Q. Liu, C. Zeng, H.K. Zhao, K.W. Xiang, Z.S. Hou, H.S. Wen, J.F. Li, Transcriptome analysis of liver, gill and intestine in rainbow trout (*Oncorhynchus mykiss*) symptomatically or asymptomatically infected with *Vibrio anguillarum*, Fish Shellfish Immunol. 135 (2023) 108643.
[46] X.D. Yang, Z.S. Hou, M.Q. Liu, C. Zeng, H.K. Zhao, Y.R. Xin, K.W. Xiang, Q. Yang, H.S. Wen, J.F. Li, Identification and characterization of mkk genes and their expression profiles in rainbow trout (*Oncorhynchus mykiss*) symptomatically or asymptomatically infected with *Vibrio anguillarum*, Fish Shellfish Immunol. 121 (2022) 1–11.
[47] D. Kim, B. Langmead, S.L. Salzberg, HISAT: a fast spliced aligner with low memory requirements, Nat. Methods 12 (2015) 357–360.
[48] Y. Liao, G.K. Smyth, W. Shi, FeatureCounts: an efficient general purpose program for assigning sequence reads to genomic features, Bioinformatics 30 (2014) 923–930.
[49] M.I. Love, W. Huber, S. Anders, Moderated estimation of fold change and dispersion for RNA-seq data with DESeq2, Genome Biol. 15 (2014) 1–21.
[50] C. Li, F. Liu, X. Li, X. Yang, Q. Li, J. Huang, Transcriptome landscape of the adrenal gland and superior cervical ganglion from hypertension-induced left ventricular hypertrophy rat model, BMC Genom. 26 (2025).
[51] K.J. Livak, T.D. Schmittgen, Analysis of relative gene expression data using real-time quantitative PCR and the $2^{-\Delta\Delta CT}$ method, Methods 25 (2001) 402–408.
[52] J. Pandit, A. Bohm, J. Jancarik, R. Halenbeck, K. Koths, S.H. Kim, Three-dimensional structure of dimeric human recombinant macrophage colony-stimulating factor, Science 258 (1992) 1358–1362.
[53] M.O. Glocker, B. Arbogast, M.L. Deinzer, J. Schreurs, Assignment of the Inter- and intramolecular disulfide linkages in recombinant human macrophage colony stimulating factor using fast atom bombardment mass spectrometry, Biochemistry 32 (1993) 482–488.
[54] C.P. Hill, T.D. Osslund, D. Eisenberg, The structure of granulocyte-colony-stimulating factor and its relationship to other growth factors, Proc. Natl. Acad. Sci. 90 (1993) 5167–5171.
[55] D.N. Silva, B.S.F. Souza, J.F. Vasconcelos, C.M. Azevedo, C.X.R. Valim, B. D. Paredes, V.P.C. Rocha, G.B. Carvalho, P.S. Daltro, S.G. Macambira, et al., Granulocyte-colony stimulating factor-overexpressing mesenchymal stem cells exhibit enhanced immunomodulatory actions through the recruitment of suppressor cells in experimental chagas disease cardiomyopathy, Front. Immunol. 9 (2018).
[56] H. he Du, H. qin Huang, K. wei Si, H. fu Dai, Y. hua Hu, Granulocyte colony stimulating factor (GCSF) of Japanese flounder (*Paralichthys olivaceus*): immunoregulatory property and anti-infectious function, Fish Shellfish Immunol. 89 (2019) 27–34.
[57] S. Peddie, J. Zou, C.J. Secombes, A biologically active IL-1β derived peptide stimulates phagocytosis and bactericidal activity in rainbow trout, *Oncorhynchus mykiss* (Walbaum), head kidney leucocytes *in vitro*, J. Fish. Dis. 25 (2002) 351–360.
[58] X. Wang, J. Chen, R. Zhang, L. Liu, G. Ma, H. Zhu, Interleukin-6 in Siberian sturgeon (*Acipenser baeri*): molecular characterization and immune functional activity, Fish Shellfish Immunol. 102 (2020) 296–306.
[59] Y. Cho, R. Joshi, P. Lowe, C. Copeland, M. Ribeiro, C. Morel, D. Catalano, G. Szabo, Granulocyte colony-stimulating factor attenuates liver damage by M2 macrophage polarization and hepatocyte proliferation in alcoholic hepatitis in mice, Hepatol. Commun. 6 (2022) 2322–2339.
[60] C. Engelmann, V. Di Martino, A.J.C. Kerbert, D. Weil-Verhoeven, N.F. Aehling, A. Herber, T. Thévenot, T. Berg, The current status of granulocyte-colony stimulating factor to treat acute-on-chronic liver failure, Semin. Liver Dis. 41 (2021) 298–307.
[61] S. Sarah, L.J. Smith, C. Penny, P. Huntington, B.T. D, T.K. L, Treatment with granulocyte-macrophage colony-stimulating factor reduces viral titers in the brains of west nile virus-infected mice and improves survival, J. Virol. 97 (2023) e01805, 22.
[62] M.S. Lionakis, R.A. Drummond, T.M. Hohl, Immune responses to human fungal pathogens and therapeutic prospects, Nat. Rev. Immunol. 23 (2023) 433–452.
[63] A. Meyer, Y. Van De Peer, From 2R to 3R: evidence for a fish-specific genome duplication (FSGD), Bioessays 27 (2005) 937–945.
[64] S.M.K. Glasauer, S.C.F. Neuhauss, Whole-genome duplication in teleost fishes and its evolutionary consequences, Mol. Genet. Genom. 289 (2014) 1045–1060.
[65] Z.S. Hou, M.Q. Liu, H.S. Wen, Q.F. Gao, Z. Li, X.D. Yang, K.W. Xiang, Q. Yang, X. Hu, M.Z. Qian, et al., Identification, characterization, and transcription of serotonin receptors in rainbow trout (*Oncorhynchus mykiss*) in response to bacterial infection and salinity changes, Int. J. Biol. Macromol. 249 (2023).
[66] J. Oltova, O. Svoboda, P. Bartunek, Hematopoietic cytokine gene duplication in zebrafish erythroid and myeloid lineages, Front. Cell Dev. Biol. 6 (2018) 1–8.
[67] A. Ogawa, S. Konno, S. Ansai, K. Naruse, T. Kato, Structural diversity and function of the granulocyte colony-stimulating factor in medaka fish, Exp. Hematol. 141 (2024) 104672.
[68] A. Theyab, M. Algahtani, K.F. Alsharif, Y.M. Hawsawi, A. Alghamdi, A. Alghamdi, J. Akinwale, New insight into the mechanism of granulocyte colony-stimulating factor (G-CSF) that induces the mobilization of neutrophils, Hematol. (United Kingdom) 26 (2021) 628–636.
[69] H. Link, Current state and future opportunities in granulocyte colony-stimulating factor (G-CSF), Support. Care Cancer 30 (2022) 7067–7077.
[70] W. Li, X. Guan, B. Sun, L. Sun, A novel microRNA of Japanese flounder regulates antimicrobial immunity involving a bacteria-binding CSF3, Front. Immunol. 12 (2021).
[71] H. Li, Z. Wang, X. Li, G-CSF as a potential early biomarker for diagnosis of bloodstream infection, J. Clin. Lab. Anal. 35 (2021) e23592.
[72] N.A. Nicola, D. Metcalf, M. Matsumoto, G.R. Johnson, Purification of a factor inducing differentiation in murine myelomonocytic leukemia cells. Identification as granulocyte colony-stimulating factor, J. Biol. Chem. 258 (1983) 9017–9023.
[73] A. Yaparla, E.S. Wendel, L. Grayfer, The unique myelopoiesis strategy of the amphibian *Xenopus laevis*, Dev. Comp. Immunol. 63 (2016) 136–143.
[74] A. Ogawa, R. Yamagishi, T. Matsumoto, S. Ansai, K. Naruse, T. Kato, The expression and role of multiple forms of granulocyte colony-stimulating factor in medaka fish, Blood 136 (2020) 35–36.
[75] J. S Cullor, N. Fairley, W. L Smith, S. L Wood, J. D Dellinger, M. S Inokuma, L. M Souza, Hemogram changes in lactating dairy cows given human recombinant granulocyte colony stimulating factor (r-MethuG-CSF), Vet. Pathol. 27 (1990) 311–316.
[76] G.J. Lieschke, D. Grail, G. Hodgson, D. Metcalf, E. Stanley, C. Cheers, K.J. Fowler, S. Basu, Y.F. Zhan, A.R. Dunn, Mice lacking granulocyte colony-stimulating factor have chronic neutropenia, granulocyte and macrophage progenitor cell deficiency, and impaired neutrophil mobilization, Blood 84 (1994) 1737–1746.
[77] S. Nagata, Gene structure and function of granulocyte colony-stimulating factor, Bioessays 10 (1989).
[78] P. Xia, Y. Wu, S. Lian, L. Yan, X. Meng, Q. Duan, G. Zhu, Research progress on toll-like receptor signal transduction and its roles in antimicrobial immune responses, Appl. Microbiol. Biotechnol. 105 (2021) 5341–5355.
[79] L.M. Pezzanite, L. Chow, V. Johnson, G.M. Griffenhagen, L. Goodrich, S. Dow, Toll-like receptor activation of equine mesenchymal stromal cells to enhance antibacterial activity and immunomodulatory cytokine secretion, Vet. Surg. 50 (2021) 858–871.
[80] S. Carpenter, L.A.J. O'Neill, How important are toll-like receptors for antimicrobial responses? Cell. Microbiol. 9 (2007) 1891–1901.
[81] G. Pei, A. Dorhoi, NOD-like receptors: guards of cellular homeostasis perturbation during infection, Int. J. Mol. Sci. (2021) 22.
[82] J. Le, Y. Kulatheepan, S. Jeyaseelan, Role of toll-like receptors and nod-like receptors in acute lung infection, Front. Immunol. 14 (2023).
[83] Z. Chen, X. Xu, J. Wang, Q. Zhou, S. Chen, A genome-wide survey of NOD-like receptors in Chinese tongue sole (*Cynoglossus semilaevis*): identification, characterization and expression analysis in response to bacterial infection, J. Fish. Biol. 99 (2021) 1786–1797.
[84] M. Sharma, P. Wagh, T. Shinde, D. Trimbake, A.S. Tripathy, Exploring the role of pattern recognition receptors as immunostimulatory molecules, immunity, Inflamm. Dis. 13 (2025) e70150.
[85] R. Alghsham, Z. Rasheed, A. Shariq, A.S. Alkhamiss, F.A. Alhumaydhi, A.S. M. Aljohani, S.A. Althwab, A. Alshomar, H.T. Alhomaidan, E.M. Hamad, et al., Recognition of pathogens and their inflammatory signaling events, open access maced, J. Med. Sci. 10 (2022) 462–467.
[86] H.S. Jun, Y.M. Lee, K.D. Song, B.C. Mansfield, J.Y. Chou, G-CSF improves murine G6PC3-deficient neutrophil function by modulating apoptosis and energy homeostasis, Blood 117 (2011) 3881–3892.
[87] W. Peng, G-CSF treatment promotes apoptosis of autoreactive T cells to restrict the inflammatory cascade and accelerate recovery in experimental allergic encephalomyelitis, Exp. Neurol. 289 (2017) 73–84.